

Original Research

Knockdown of JMJD1C, a target gene of hsa-miR-590-3p, inhibits mitochondrial dysfunction and oxidative stress in MPP⁺-treated MES23.5 and SH-SY5Y cells

J. Wang*, T. Le, R. Wei, Y. Jiao

Department of Neurology, the Second Affiliated Hospital of Zhengzhou University, NO.2 Jingba Road, Zhengzhou 450014, Henan Province, P. R. China

Abstract: MicroRNAs have been shown to be closely related to many neurodegenerative disorders. The present study focuses on the role of hsa-miR-590-3p and its function in Parkinson's disease (PD). Our study showed a remarkable down-regulation of miR-590-3p expression in the 1-methyl-4 phenylpyridinium (MPP⁺)-treated MES23.5 and SH-SY5Y cells. Furthermore, JMJD1C was identified as a target gene of miR-590-3p in humans via the luciferase reporter assay. Our study also demonstrated that up-regulation of miR-590-3p and knockdown of JMJD1C increased the expression of peroxisome proliferator-activated receptor γ coactivator-1 α (PGC-1 α) and the downstream targets of PGC-1 α , including nuclear respiratory factor 1 (NRF-1) and mitochondrial transcription factor A (TFAM), which are the key genes regulating mitochondrial function. Also, the expression of heme oxygenase-1 (HO-1), NAD (P) H quinone oxidoreductase-1 (NQO-1) and γ -glutamylcysteine synthetase (γ -GCS) involved in anti-oxidation was increased. Moreover, there was a significant increase in the total cellular ATP with an associated decrease in levels of ROS in the absence of JMJD1C. Taken together, these results show that miR-590-3p plays an important role in the pathogenesis of PD, which may be further regarded as a therapeutic target.

Key words: Parkinson's disease, hsa-miR-590-3p, JMJD1C, mitochondrial functions, oxidative stress.

Introduction

Parkinson's disease (PD) affects 1%-2% of the world's population and is the second most common neurodegenerative disease (1). The morbidity is about 1% in the population over 65 years old, and increases to 4% for those over 85 years old (2). The main symptoms of PD, including bradykinesia, rigidity, static tremor, cognitive/mental abnormality etc., are mainly due to the progressive death of dopaminergic neurons in the substantia nigra *pars compacta* (SN) (3), causing a remarkable reduction of dopamine (DA) levels (4), which leads to an imbalance between DA and acetyl choline (ACH) in SN. This imbalance may lead to cell dysfunction and neuron death. The pathogenesis of PD is still not fully clear and there is no cure.

Oxidative stress is a kind of stress response due to the imbalance between oxidation and anti-oxidation (5). The tendency to oxidation contributes to the pathogenesis of aging and various diseases, and the magnitude of oxidative stress is related to the ability of cellular antioxidants that neutralize the accumulating reactive oxygen species (ROS) (6). The excessive ROS may cause the oxidative degradation of DNA, protein, and lip to destruct the intracellular formation and functions, mainly due to their high activity (7). Brain tissue is particularly susceptible to oxidative stress, because the brain needs more oxygen to produce adenosine triphosphate (ATP), and ROS is the reduction product (8). Furthermore, ROS may lead to a cumulative effect because of the non-regeneration of neurons. Neurons are energy-consuming due to their quick response to surroundings and stimuli, and require a mass of mitochondria to produce plenty of ATP; hence, mitochondrial dysfunction easily causes neuronal dysfunction and degeneration (9). As a result, mitochondrial dysfunction is

a key reason for PD, which is also a major pathological manifestation of PD. In sum, mitochondrial dysfunction and oxidative stress are thought to contribute to the pathogenesis of PD (10, 11). In particular, there is clear anatomical evidence that PD brains, particularly in the SN, have consistently showed mitochondrial dysfunction and increased levels of oxidative stress (12-14).

MicroRNAs (miRNAs) are a group of small, single-stranded and non-coding RNAs, which have been identified as post-transcriptional regulators of gene expression (15). Previous studies have demonstrated that miRNAs are pathologically altered in the progress of neurodegenerative diseases (16). For example, Vallelunga *et al.* have observed that miR-339-5p was down-regulated, but miR-223, miR-324-3p, miR-24 were up-regulated in PD tissues, which may be regarded as specific diagnosis biomarkers of PD (17). Burgos *et al.* investigated the miRNAs in the cerebrospinal fluid and serum, and found that 13 novel miRNAs could be used to assess disease progression and therapeutic efficacy (18). In addition, miR-34b/c expression was identified to be decreased in brain samples from PD patients compared with healthy samples (19). JMJD1C is a H3K9 demethylase, which has previously been shown to control the balance of histone methylation status through interactions with histone methyltransferases and WHISTLE for transcriptional regulation (20). The bioinformatic analysis showed that JMJD1C was a target gene of hsa-miR-590-3p,

Received December 22, 2015; Accepted March 15, 2016; Published March 20, 2016

* Corresponding author: Jinlan Wang, Department of Neurology, the Second Affiliated Hospital of Zhengzhou University, No. 2, Jingba Road, Zhengzhou 450014, Henan Province, P. R. China. Email: jinlanwangedu@163.com

Copyright: © 2016 by the C.M.B. Association. All rights reserved.

which needed further verification in the present study.

Here, we have confirmed the down-regulated expression of miR-590-3p in the PD model of MPP⁺-treated MES23.5 and SH-SY5Y cells. Subsequently, JMJD1C was identified as a target gene of miR-590-3p, participating in the regulation of mitochondrial function and oxidative stress. More specifically, knockdown of JMJD1C could inhibit mitochondrial dysfunction, and reduce the ROS level, which may be a better therapeutic target for PD.

Materials and Methods

Cell culture

Human MES23.5 and SH-SY5Y cells were purchased from the American Type Culture Collection (ATCC, Rockville, MD, USA) and cultured in DMEM (Hyclone, Logan, UT, USA) supplemented with 10% FBS (Hyclone) in an atmosphere of 37 °C with 5% CO₂. The medium was changed every two days. The cell cultures were rinsed with pre-warmed phosphate-buffered saline (PBS) before they were dissociated using Trypsin-EDTA Solution (Hyclone).

Cell treatment protocol

MES23.5 and SH-SY5Y cells were cultured and treated with 200 μM 1-methyl-4 phenylpyridinium (MPP⁺, Sigma-Aldrich, St. Louis, MO, USA) following a previous dose effect study (21).

Lentivirus construction and transfection

The lentivirus gene transfer vector of hsa-miR-590-3p was constructed by GenePharma Co., Ltd. (Shanghai, China). Scramble lentivirus was regarded as the negative control. Briefly, the lentiviruses were diluted in a complete medium containing polybrene (8 mg/ml) and added to the MES23.5 and SH-SY5Y cells for 12 h of incubation at 37 °C. This was followed by another 24 h of incubation with freshly prepared polybrene-DMEM, which was replaced with fresh DMEM for another 3 days of culture. Subsequently, the miR-590-3p expression was measured by real-time quantitative PCR.

Luciferase reporter assay

The possible binding sites of miR-590-3p in 3'-untranslated regions (3'-UTR) of JMJD1C gene were predicted using bioinformatic methods (microRNA.org, <http://www.microRNA.org/microRNA/home.do/>). Firstly, the complementary DNA (cDNA) fragments containing the predicted miR-590-3p binding sites in JMJD1C gene were amplified and subcloned into pmirGLO Dual-Luciferase miRNA Target Expression Vector (Promega, Madison, WI, USA; named pmirGLO-JMJD1C). The mutated plasmids were also constructed using cDNA fragments containing corresponding mutated nucleotides for miR-590-3p binding sites (named pmirGLO-mutJMJD1C). The pre-miR-590-3p and pre-miR-scramble plasmids were constructed and amplified in preparation for use. HEK-293T cells were digested using Trypsin-EDTA Solution (Hyclone) and seeded into 24-well plates with a density of 2 × 10⁵ cells/well, followed by incubation in 37 °C with 5% CO₂ for 24 h to reach a confluence of 80%. Subsequently, HEK-293T cells were co-transfected with either pmirGLO-

JMJD1C (100 ng/well) or pmirGLO-mutJMJD1C (100 ng/well) in the presence of either pre-miR-590-3p (50 nmol/L) or pre-miR-scramble (50 nmol/L) using LipofectamineTM 2000 Reagent (Invitrogen, Carlsbad, CA, USA) and incubated for another 48 h. The cells were harvested and the luciferase activities were measured using the Dual-Luciferase Reporter Assay Kit (Promega) according to the manufacturer's instructions.

Small interfering RNA (siRNA) transfections

JMJD1C siRNA (Invitrogen) was used in the present study, and the sequence for the 3'-UTR was 5'-GCAC-CAGTCACCTCATCTT-3'. A scramble siRNA (Invitrogen) was used as the negative control, and the sequence for the 3'-UTR was 5'-GCATGACACCTC-TACCCTT-3'. Briefly, MES23.5 and SH-SY5Y cells were transfected with siRNAs using LipofectamineTM 2000 Reagent (Invitrogen) according to the manufacturer's instructions. The effects of transfections were determined by JMJD1C expression 48 h after transfection via quantitative PCR and Western blot, respectively.

RNA extraction and real-time quantitative PCR

Total RNA was collected using the TRIzol[®] Plus RNA Purification Kit (Ambion, Rockville, MD, USA) following the manufacturer's instructions. RNA was quantified using the spectrophotometer at 260 nm, and cDNA was synthesized using the Thermo Scientific RevertAid First Strand cDNA Synthesis Kit (Thermo Fisher Scientific, Waltham, MA, USA). The synthesized cDNA was then diluted three-fold in sterile water and stored at -20 °C in preparation for PCR analysis. Real-time quantitative PCR was performed using the SYBR[®] Premix Ex TaqTM (Takara Biotechnology, Dalian, China) and Bio-Rad CFX96 touch q-PCR system (Bio-Rad, Hercules, CA, USA). Briefly, 1 μl of cDNA was mixed with 5 μl of SYBR[®] Premix Ex TaqTM, 1 μl of forward primer, 1 μl of reverse primer, and 1 μl of sterile water. β-actin served as an internal reference gene for non-microRNAs molecules, and U6 small nuclear RNA (snRNA) for miR-590-3p. The 2^{-ΔΔCt} method was employed to calculate the fold induction. The primer sequences involved in this study were shown in Table 1.

Western blot

RIPA buffer (Sigma-Aldrich) was used to collect the protein according to the manufacturer's instructions. Bradford's method was used to estimate the protein concentration. The target protein was then separated by sodium dodecyl sulfate-polyacrylamide gel electrophoresis (SDS-PAGE). Subsequently, protein bands were electro-blotted onto polyvinylidene difluoride (PVDF) membranes (Invitrogen) and were blocked with 10% (w/v) bovine serum albumin (BSA) overnight at 4 °C. The membranes were then incubated for 2 h at room temperature with primary antibodies, including mouse anti-JMJD1C (sc-101073; diluted at 1:1000; Santa Cruz Biotechnology, Santa Cruz, CA, USA), mouse anti-HO-1 (sc-136960; diluted at 1:1500; Santa Cruz Biotechnology), rabbit anti-NQO-1 (AB10239; diluted at 1:800; Merck Millipore, Billerica, MA, USA), rabbit anti-γ-GCS (PA1-37756; diluted at 1:200; Thermo Fisher Scientific, Waltham, MA, USA), goat anti-PGC-1α (ab106814; diluted at 1:1000; Abcam, Cam-

Table 1. The primer sequences used in this study

Gene	Primer sequences (5'-3')	Product
MiR-590-3p	Forward: TAGCCAGTCAGAAATGAGCTT Reverse: TGCTGCATGTTTCAATCAGAGA	97 bp
JMJD1C	Forward: TCTGCCACCCAGTGGTTTAC Reverse: TTGGGCACGTGTATAATGGCT	243 bp
HO-1	Forward: TTCAAGCAGCTCTACCGCTC Reverse: TCTTGCACTTTGTTGCTGGC	206 bp
NQO-1	Forward: GGTTTGGAGTCCCTGCCATT Reverse: GCCTTCTTACTCCGGAAGGG	112 bp
γ -GCS	Forward: ACTTCATTTCCCAGTACCTTAACA Reverse: CCGGCTTAGAAGCCCTTGAA	154 bp
PGC-1 α	Forward: TGCATGAGTGTGTGCTCTGT Reverse: GCACACTCGATGTCACTCCA	131 bp
NRF-1	Forward: CACAGAAAAGGTGCTCAAAGGAT Reverse: TTTGGGTCACCTCCGTGTTCC	106 bp
TFAM	Forward: CTCCGCAGGCTAGAGGATTG Reverse: CACTAGCGAGGCACTATGGG	168 bp
β -actin	Forward: CCTCGCCTTTGCCGATCC Reverse: GGCCATCTCTTGCTCGAAGT	733 bp

bridge, UK), mouse anti-NRF-1 (sc-101102; diluted at 1:500; Santa Cruz Biotechnology), rabbit anti-TFAM (ab131607; diluted at 1:800; Abcam) and rabbit anti- β -actin (ab129348; diluted at 1:1500; Abcam), followed by incubation with horseradish peroxidase (HRP)-conjugated secondary antibodies (Invitrogen), including goat anti-mouse IgG (A24518; diluted at 1:4000), goat anti-rabbit IgG (A24537; diluted at 1:4000) and rabbit anti-goat IgG (A24452; diluted at 1:4000) antibodies. Specific binding was revealed by enhanced chemiluminescence (ECL) detection system (Amersham, Little Chalfont, UK). The densitometry analysis was performed using Image-Pro Plus 7.0 (Roper Industries, New York, NY, USA).

Measurement of extracellular ROS assay

The amount of ROS was estimated using the Reactive Oxygen Species Assay Kit (Beyotime, Jiangsu, China). Briefly, dichlorodihydrofluorescein-diacetate (DCFH-DA) was diluted at 1:1000 to a concentration of 10 μ M. Subsequently, around 1 ml of diluted DCFH-DA was added to a 6-well plate, from which the medium had been removed, and incubated for 20 min at 37 °C. The Rosup served as positive control instead of DCFH-DA. After incubation, the cells were washed with non-serum medium three times to wipe out the dissociative DCFH-DA. The fluorescence of the controls and samples was read at 488-nm excitation/525-nm emissions using a Fluoview FV1000 laser scanning confocal microscope (Olympus, Osaka, Japan). The generated dichlorodihydrofluorescein (DCF) standard curve was used to calculate the concentration of total ROS.

Measurement of intracellular ATP

ATP levels in the MES23.5 and SH-SY5Y cells before and after treatment were measured using the ATP Assay Kit (Beyotime) according to the manufacturer's instructions. Briefly, 200 μ l of cell lysis solution was added to a 6-well plate, with occasional shaking. Next, the lysates were centrifuged with 12,000 r/min at 4 °C for 5 min and the supernatants were collected as samples. The standard curve and ATP detection reagent were also prepared. Subsequently, 100 μ l of detection reagent was added into a centrifuge tube and kept for 5 min at room

temperature to consume its own ATP. The samples were then added to the tube and mixed immediately, and the relative light units were measured using a GloMaxTM 96 Microplate Luminometer (Promega). The standard curve was used to calculate the ATP concentration.

MTT assay

Cell viability was measured using the MTT Cell Proliferation and Cytotoxicity Assay Kit (Beyotime) following manufacturer's instructions. Briefly, MES23.5 and SH-SY5Y cells were digested and seeded into 96-well plates with a density of 1×10^4 cells/well, which were then subjected to intended conditions as described above. Subsequently, 20 μ l of MTT solution was added to each well. Cells were incubated with MTT for 4 h, and the medium was then discarded. Dimethylsulfoxide was added to dissolve formed formazan, and the optical density (OD) value was measured at 490 nm using the GloMaxTM 96 Microplate Luminometer (Promega).

Statistical analysis

The data was represented as mean \pm standard deviation (SD). One-way ANOVA and Student's t-test was used to calculate the statistical significance between groups; * $p < 0.05$ and ** $p < 0.01$ represented the statistical significance.

Results

MiR-590-3p is down-regulated in MPP⁺-treated MES23.5 and SH-SY5Y cells

As shown in Figs. 1A and B, after treatment with MPP⁺ in MES23.5 and SH-SY5Y cells, the expression of miR-590-3p was significantly inhibited, indicating that miR-590-3p expression was down-regulated in PD.

JMJD1C is one of the target genes of hsa-miR-590-3p

To further identify the specific function of miR-590-3p in PD, we aimed to uncover the target gene. As shown in Fig. 2A, miR-590-3p expression was significantly increased after lentivirus-mediated transfection both in MES23.5 and SH-SY5Y cells. The binding sites of miR-590-3p in the 3'-UTR of original and mutated JMJD1C

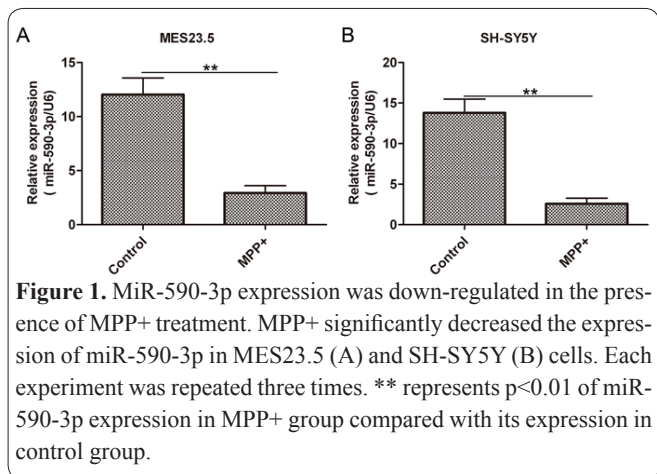


Figure 1. MiR-590-3p expression was down-regulated in the presence of MPP+ treatment. MPP+ significantly decreased the expression of miR-590-3p in MES23.5 (A) and SH-SY5Y (B) cells. Each experiment was repeated three times. ** represents $p < 0.01$ of miR-590-3p expression in MPP+ group compared with its expression in control group.

JMJD1C protein expression is down-regulated by miR-590-3p overexpression, but up-regulated by MPP+ treatment

Since JMJD1C was the target gene of miR-590-3p, we wanted to further investigate the effects of MPP+ treatment and miR-590-3p overexpression on JMJD1C expression. Interestingly, as shown in Figs. 3A and B, the JMJD1C expression was not significantly altered in the mRNA level via PCR analysis. Western blot results showed that in the protein level, the MPP+ treatment significantly promoted the JMJD1C protein expression, whereas miR-590-3p overexpression markedly inhibited the protein expression (Figs. 3C and D), indicating that miR-590-3p was a negative regulator of JMJD1C. The corresponding densitometry analysis of Western blots was shown in Figs. 3E and F.

JMJD1C expression is inhibited by siRNA transfections

As shown in Figs. 4A and B, the expression of JMJD1C had a sharp decrease in JMJD1C siRNA group

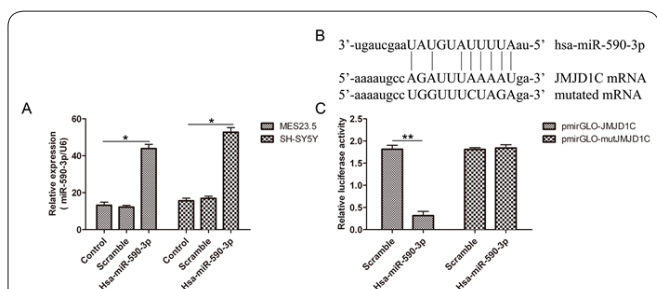


Figure 2. JMJD1C was the target gene of miR-590-3p. (A) MiR-590-3p expression was significantly increased by lentivirus-mediated transfections of hsa-miR-590-3p in both MES23.5 and SH-SY5Y cells. (B) Hsa-miR-590-3p had some binding sites in the 3'-UTR of JMJD1C, rather than the mutated JMJD1C. (C) MiR-590-3p overexpression remarkably inhibited the transcription of Luciferase reporter containing miR-590-3p binding sites, but didn't affect the one with mutated binding sites. Each experiment was repeated three times. * represents $p < 0.05$ of miR-590-3p expression in hsa-miR-590-3pMPP+ group compared with its expression in control group in (A); ** represents $p < 0.01$ of luciferase activity in hsa-miR-590-3p group compared with that in scramble group.

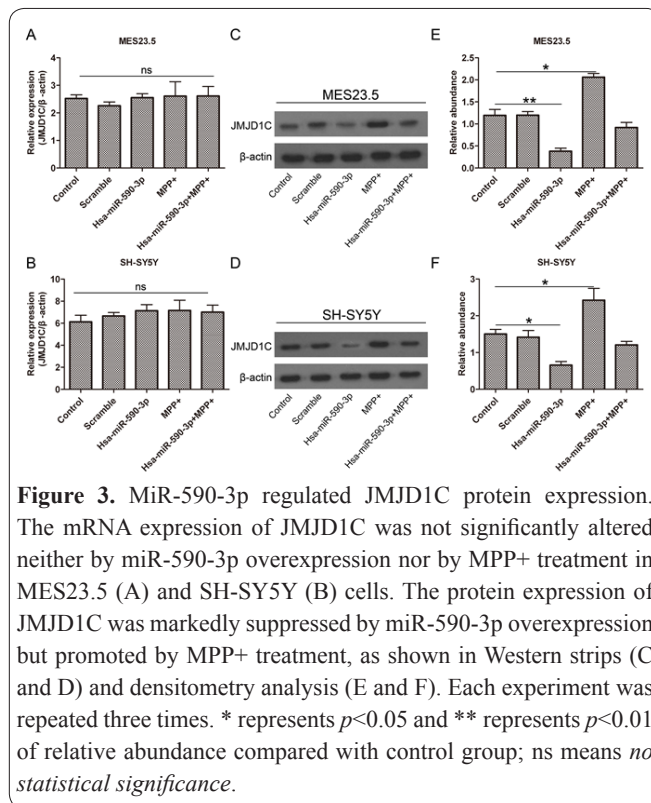


Figure 3. MiR-590-3p regulated JMJD1C protein expression. The mRNA expression of JMJD1C was not significantly altered neither by miR-590-3p overexpression nor by MPP+ treatment in MES23.5 (A) and SH-SY5Y (B) cells. The protein expression of JMJD1C was markedly suppressed by miR-590-3p overexpression but promoted by MPP+ treatment, as shown in Western strips (C and D) and densitometry analysis (E and F). Each experiment was repeated three times. * represents $p < 0.05$ and ** represents $p < 0.01$ of relative abundance compared with control group; ns means *no statistical significance*.

in mRNA level compared with control and scramble siRNA groups, no matter in the presence or absence of MPP+ treatment. In other words, MPP+ did not play a role if JMJD1C was knocked down. The protein expression of JMJD1C (Figs. 4C and D) was similar with mRNA results and its densitometry analysis was shown in Figs. 4E and F.

ROS level is decreased upon the lowly expressed JMJD1C

ROS level was measured to assess oxidative stress. As shown in Fig. 4G, the ROS level was significantly reduced by JMJD1C knockdown and miR-590-3p overexpression, indicating that the low expression of JMJD1C led to decreased expression of ROS. In contrast, MPP+ treatment significantly increased the ROS level (Fig. 4G). Taken together, these results demonstrated that knockdown of JMJD1C contributed to the antioxidative effects, and that the effects of MPP+ and miR-590-3p overexpression depended on the regulation of JMJD1C expression.

ATP level is increased upon the lowly expressed JMJD1C

The level of ATP is a reflection of mitochondrial function. As shown in Fig. 5B, there was a significant decrease in the level of ATP after MPP+ treatment. However, this inhibitory effect was reversed by miR-590-3p overexpression (Fig. 4H). It is also worth noting that the knockdown of JMJD1C increased the ATP level significantly, indicating that JMJD1C was a negative regulator of mitochondrial function.

Knockdown of JMJD1C increases the expression of heme oxygenase-1 (HO-1), NAD (P) H quinone oxidoreductase-1 (NQO-1) and γ -glutamylcysteine synthetase (γ -GCS)

Since the ROS level was reduced by JMJD1C silen-

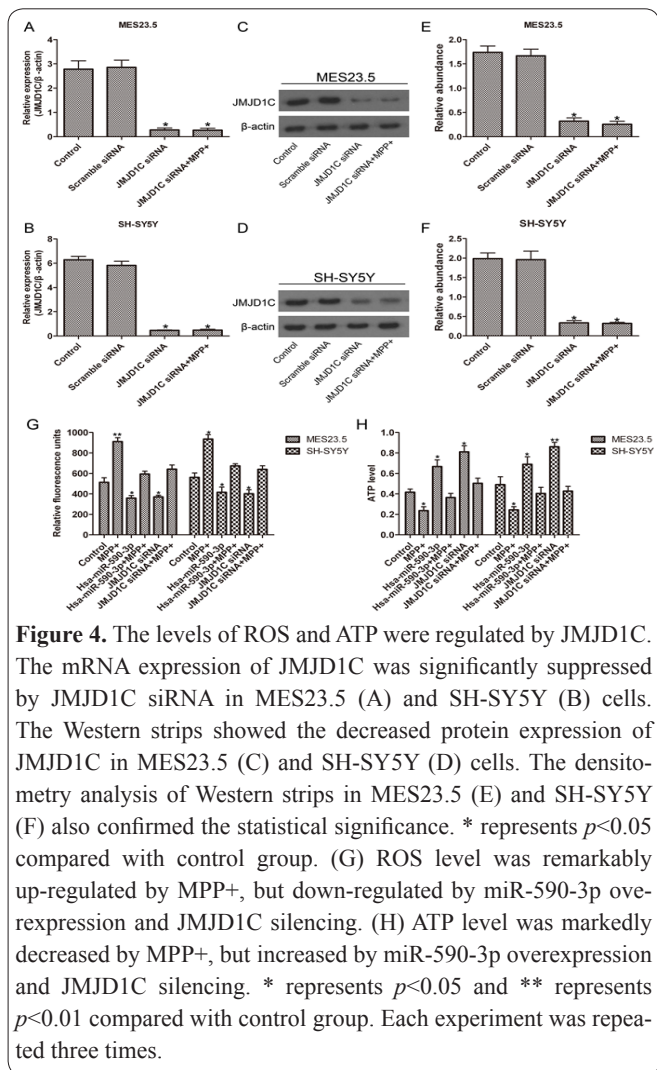


Figure 4. The levels of ROS and ATP were regulated by JMJD1C. The mRNA expression of JMJD1C was significantly suppressed by JMJD1C siRNA in MES23.5 (A) and SH-SY5Y (B) cells. The Western strips showed the decreased protein expression of JMJD1C in MES23.5 (C) and SH-SY5Y (D) cells. The densitometry analysis of Western strips in MES23.5 (E) and SH-SY5Y (F) also confirmed the statistical significance. * represents $p < 0.05$ compared with control group. (G) ROS level was remarkably up-regulated by MPP⁺, but down-regulated by miR-590-3p overexpression and JMJD1C silencing. (H) ATP level was markedly decreased by MPP⁺, but increased by miR-590-3p overexpression and JMJD1C silencing. * represents $p < 0.05$ and ** represents $p < 0.01$ compared with control group. Each experiment was repeated three times.

Knockdown of JMJD1C increases the expression of peroxisome proliferator-activated receptor γ coactivator-1 α (PGC-1 α), nuclear respiratory factor 1 (NRF-1) and mitochondrial transcription factor A (TFAM)

Similarly, the mitochondrial function-related genes were also investigated. The down-regulation of JMJD1C showed a promotive effect on the expression of PGC-1 α , NRF-1 and TFAM, which reversed the effects of MPP⁺ on their expression in both the mRNA level (Figs. 6A, C and E) and protein level (Figs. 6B, D and F). Moreover, MPP⁺ treatment significantly decreased the expression of PGC-1 α , NRF-1 and TFAM. These results indicated that knockdown of JMJD1C increased mitochondrial function possibly through up-regulating PGC-1 α , NRF-

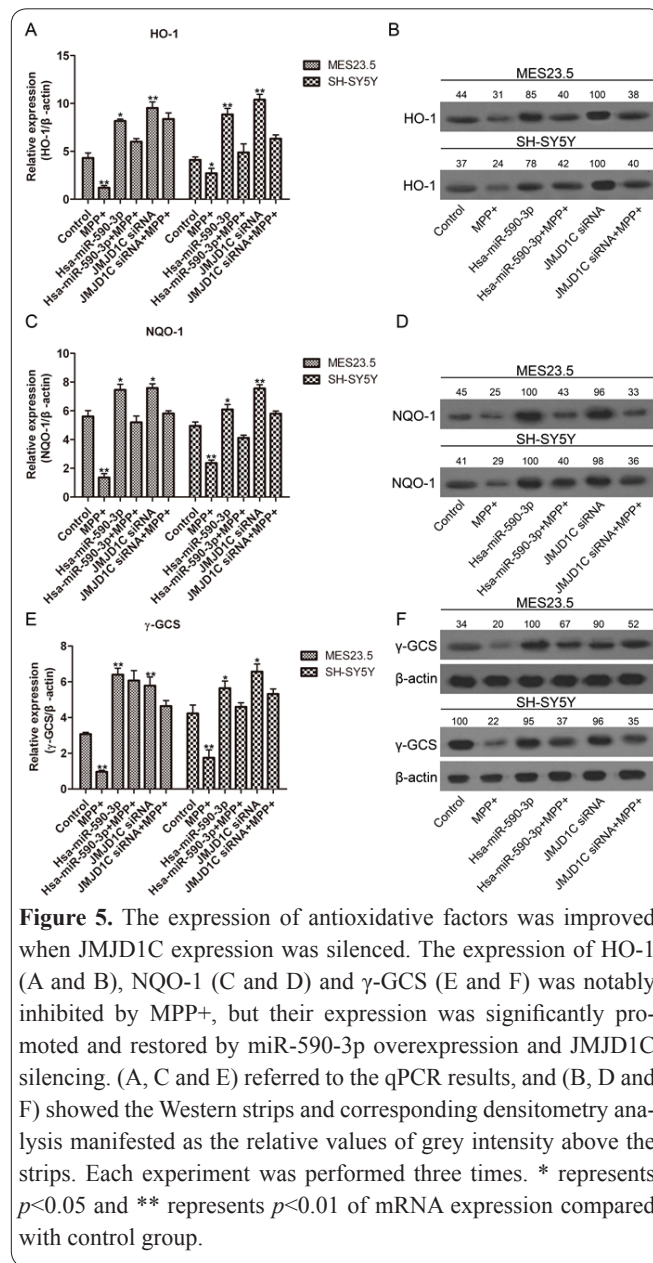


Figure 5. The expression of antioxidative factors was improved when JMJD1C expression was silenced. The expression of HO-1 (A and B), NQO-1 (C and D) and γ -GCS (E and F) was notably inhibited by MPP⁺, but their expression was significantly promoted and restored by miR-590-3p overexpression and JMJD1C silencing. (A, C and E) referred to the qPCR results, and (B, D and F) showed the Western strips and corresponding densitometry analysis manifested as the relative values of grey intensity above the strips. Each experiment was performed three times. * represents $p < 0.05$ and ** represents $p < 0.01$ of mRNA expression compared with control group.

MiR-590-3p overexpression and JMJD1C siRNA protect cells against MPP⁺

As shown in Fig. 7, MPP⁺ treatment significantly decreased cell viability, both in MES23.5 (A) and SH-SY5Y (B) cells. Moreover, miR-590-3p overexpression and knockdown of JMJD1C markedly restored cell viability compared with MPP⁺ group. These results demonstrated that the genetic interventions indeed protected MES23.5 and SH-SY5Y cells against MPP⁺, which would be a promising pharmacological method against PD.

Discussion

In the present study, hsa-miR-590-3p was found to be down-regulated in MPP⁺-treated MES23.5 and SH-SY5Y cells. MPP⁺ is a kind of positively charged compound, which may affect the process of oxidative phosphorylation in mitochondria (22), leading to the over-consumption of ATP and cell death (23). Hence, MPP⁺ is a contaminator of mitochondrial functions. It is feasible to mimic PD with the treatment of MPP⁺

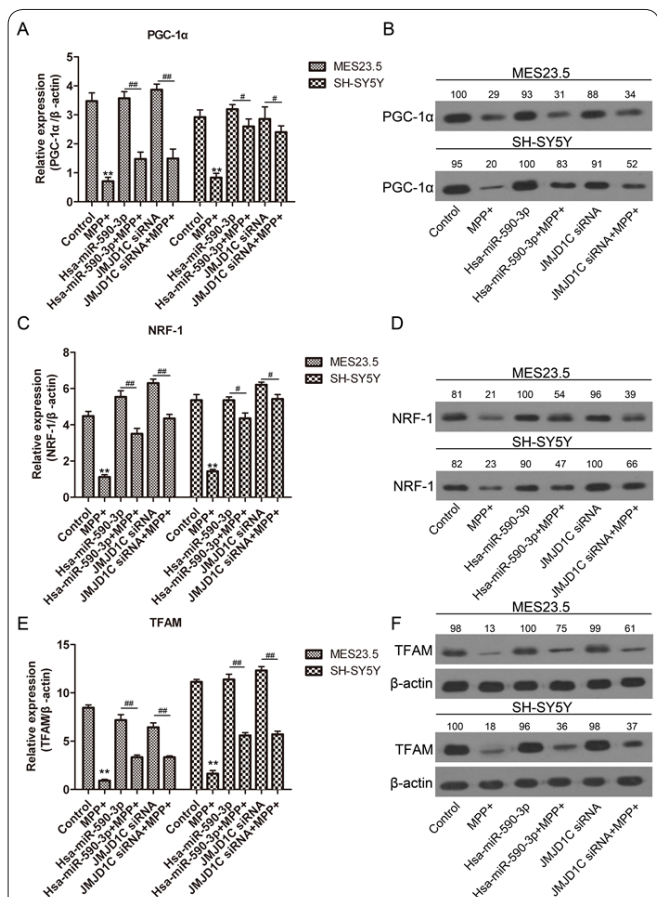


Figure 6. The expression of mitochondrial function-related genes was improved when JMJD1C expression was silenced. The expression of PGC-1α (A and B), NRF-1 (C and D) and TFAM (E and F) was markedly suppressed by MPP⁺, but their expression was significantly enhanced and restored by miR-590-3p overexpression and JMJD1C silencing. (A, C and E) referred to the qPCR results, and (B, D and F) showed the Western strips and corresponding densitometry analysis manifested as the relative values of grey intensity above the strips. Each experiment was performed three times. ** represents $p < 0.01$ of mRNA expression compared with control group; # represents $p < 0.05$ and ## represents $p < 0.01$ of mRNA expression compared between MPP⁺-plus and MPP⁺-free groups.

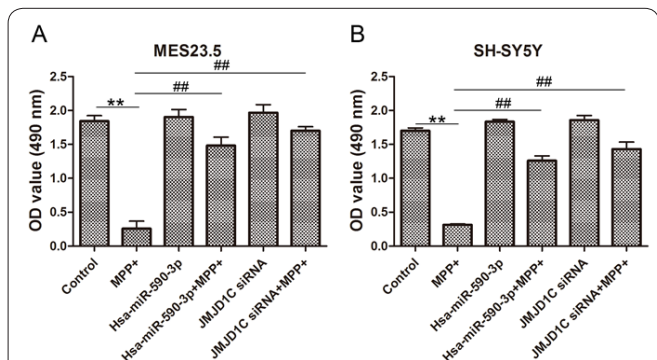


Figure 7. MiR-590-3p overexpression and knockdown of JMJD1C improved cell viability. Compared with MPP⁺ group, miR-590-3p overexpression and knockdown of JMJD1C significantly improved cell viability even in the presence of MPP⁺, demonstrating a cytoprotective effect. ** represents $p < 0.01$ of OD value in MPP⁺ group compared with control group; ## represents $p < 0.01$ of OD value compared with MPP⁺ group. Each assay was performed in 3 parallel wells.

because the main symptoms of PD are similar to the MPP⁺-caused effects as previously reported (24). As a

result, hsa-miR-590-3p down-regulation was thought to be a common phenomenon in PD model.

MiRNAs play a role in regulating physiological processes by inhibiting the expression of its target genes in post-transcriptional-translation. To explore the underlying mechanisms, the target gene of hsa-miR-590-3p had to be discovered. With the help of bioinformatic analysis via *microRNA.org* and luciferase reporter assay, JMJD1C was found to have interactions with hsa-miR-590-3p; in other words, JMJD1C was the target gene of hsa-miR-590-3p.

The oxidative stress and mitochondrial dysfunction often occur as a consequence of PD (11). To be specific, oxidative stress produces more ROS that may damage the brain tissue (25). Mitochondrial dysfunction reduces the level of ATP, leading to an insufficient supply of energy (26). The accumulating effects of “over-ROS” and “lack-ATP” cause the deaths of more dopaminergic neurons, which in turn promotes PD development. Perfeito *et al.* demonstrated that oxidative stress and mitochondrial dysfunction are similar to the effect of the abuse of amphetamine drugs, which may lead to dopamine depletion (27). Hence, we next aimed to investigate the role of miR-590-3p and JMJD1C in oxidative stress and mitochondrial dysfunction.

After MPP⁺ treatment, as shown in Figs. 5 and 6, there was a significant increase in the ROS level and decrease in the ATP level. These characteristics are similar to the symptoms of PD. More experiments were performed based on this PD model. It is worth noting that knockdown of JMJD1C could help counteract the effects of MPP⁺ in a PD model. Decreased ROS and increased ATP levels were both seen after miR-590-3p overexpression and JMJD1C knockdown, confirming the inhibition of mitochondrial dysfunction and oxidative stress. The nuclear factor E2-related factor 2 (Nrf2) is a kind of transcription factor, which could initiate antioxidant response element (ARE) transcription. Nrf2 gene products include HO-1, NQO-1 and γ -GCS (28, 29). In general, the Nrf2/ARE signaling pathway could promote the antioxidative effects—namely, the up-regulation of HO-1, NQO-1 and γ -GCS could reduce the ROS level. Similarly, PGC-1α, NRF-1 and TFAM are the key genes that promote mitochondrial function. The exploration of these genes could help understand the mechanisms underlying the role of miR-590-3p and JMJD1C in PD.

In conclusion, in this present study, with the help of the PD model, we discovered the interactions between hsa-miR-590-3p and PD. MiR-590-3p was found to be down-regulated in PD, and its target gene JMJD1C participated in the regulation of oxidative stress and mitochondrial dysfunction. Specifically, knockdown of JMJD1C may play a role in the recovery from PD, which would serve as a potential therapeutic target.

References

- de Rijk MC, Breteler MM, Graveland GA, Ott A, Grobbee DE, van der Meche FG and Hofman A, Prevalence of Parkinson's disease in the elderly: the Rotterdam Study. *Neurology*. 1995;45:2143-2146.
- de Rijk MC, Launer LJ, Berger K, Breteler MM, Dartigues JF, Baldereschi M, Fratiglioni L, Lobo A, Martinez-Lage J, Trenkwalder C and Hofman A, Prevalence of Parkinson's disease in Europe:

A collaborative study of population-based cohorts. Neurologic Diseases in the Elderly Research Group. *Neurology*. 2000,54:S21-23.

3. Fahn S, The medical treatment of Parkinson disease from James Parkinson to George Cotzias. *Mov Disord*. 2015,30:4-18.
4. Christopher L, Duff-Canning S, Koshimori Y, Segura B, Boileau I, Chen R, Lang AE, Houle S, Rusjan P and Strafella AP, Salience network and parahippocampal dopamine dysfunction in memory-impaired Parkinson disease. *Ann Neurol*. 2015,77:269-280.
5. Mota SI, Costa RO, Ferreira IL, Santana I, Caldeira GL, Padovano C, Fonseca AC, Baldeiras I, Cunha C, Letra L, Oliveira CR, Pereira CM and Rego AC, Oxidative stress involving changes in Nrf2 and ER stress in early stages of Alzheimer's disease. *Biochim Biophys Acta*. 2015,1852:1428-1441.
6. Ruskiewicz J and Albrecht J, Changes in the mitochondrial antioxidant systems in neurodegenerative diseases and acute brain disorders. *Neurochem Int*. 2015.
7. Ma J, Yuan X, Qu H, Zhang J, Wang D, Sun X and Zheng Q, The role of reactive oxygen species in morphine addiction of SH-SY5Y cells. *Life Sci*. 2015,124:128-135.
8. Pike LS, Smift AL, Croteau NJ, Ferrick DA and Wu M, Inhibition of fatty acid oxidation by etomoxir impairs NADPH production and increases reactive oxygen species resulting in ATP depletion and cell death in human glioblastoma cells. *Biochim Biophys Acta*. 2011,1807:726-734.
9. Exner N, Lutz AK, Haass C and Winklhofer KF, Mitochondrial dysfunction in Parkinson's disease: molecular mechanisms and pathophysiological consequences. *EMBO J*. 2012,31:3038-3062.
10. Gautier CA, Corti O and Brice A, Mitochondrial dysfunctions in Parkinson's disease. *Rev Neurol (Paris)*. 2014,170:339-343.
11. Yan MH, Wang X and Zhu X, Mitochondrial defects and oxidative stress in Alzheimer disease and Parkinson disease. *Free Radic Biol Med*. 2013,62:90-101.
12. Schapira AH, Etiology and pathogenesis of Parkinson disease. *Neurol Clin*. 2009,27:583-603, v.
13. Schapira AHV, Oxidative stress in Parkinson's disease. *Neuropathology and Applied Neurobiology*. 1995,21:3-9.
14. Owen AD, Schapira AHV, Jenner P and Marsden CD, Oxidative Stress and Parkinson's Disease. *Annals of the New York Academy of Sciences*. 1996,786:217-223.
15. Graves P and Zeng Y, Biogenesis of mammalian microRNAs: a global view. *Genomics Proteomics Bioinformatics*. 2012,10:239-245.
16. Tan L and Yu JT, Causes and Consequences of MicroRNA Dysregulation in Neurodegenerative Diseases. *Mol Neurobiol*. 2014.
17. Vallelunga A, Ragusa M, Di Mauro S, Iannitti T, Pilleri M, Biundo R, Weis L, Di Pietro C, De Iuliis A, Nicoletti A, Zappia M, Purrello M and Antonini A, Identification of circulating microRNAs for the differential diagnosis of Parkinson's disease and Multiple

System Atrophy. *Front Cell Neurosci*. 2014,8:156.

18. Burgos K, Malenica I, Metpally R, Courtright A, Rakela B, Beach T, Shill H, Adler C, Sabbagh M, Villa S, Tembe W, Craig D and Van Keuren-Jensen K, Profiles of extracellular miRNA in cerebrospinal fluid and serum from patients with Alzheimer's and Parkinson's diseases correlate with disease status and features of pathology. *PLoS One*. 2014,9:e94839.
19. Minones-Moyano E, Porta S, Escaramis G, Rabionet R, Iraola S, Kagerbauer B, Espinosa-Parrilla Y, Ferrer I, Estivill X and Marti E, MicroRNA profiling of Parkinson's disease brains identifies early downregulation of miR-34b/c which modulate mitochondrial function. *Hum Mol Genet*. 2011,20:3067-3078.
20. Kim S-M, Kim J-Y, Choe N-W, Cho I-H, Kim J-R, Kim D-W, Seol J-E, Lee SE, Kook H and Nam K-I, Regulation of mouse steroidogenesis by WHISTLE and JMJD1C through histone methylation balance. *Nucleic acids research*. 2010,38:6389-6403.
21. Wang J, Duhart HM, Xu Z, Patterson TA, Newport GD and Ali SF, Comparison of the time courses of selective gene expression and dopaminergic depletion induced by MPP⁺ in MN9D cells. *Neurochem Int*. 2008,52:1037-1043.
22. Tsou YH, Shih CT, Ching CH, Huang JY, Jen CJ, Yu L, Kuo YM, Wu FS and Chuang JI, Treadmill exercise activates Nrf2 antioxidant system to protect the nigrostriatal dopaminergic neurons from MPP⁺ toxicity. *Exp Neurol*. 2015,263:50-62.
23. Radad KS, Al-Shraim MM, Moustafa MF and Rausch WD, Neuroprotective role of thymoquinone against 1-methyl-4-phenylpyridinium-induced dopaminergic cell death in primary mesencephalic cell culture. *Neurosciences (Riyadh)*. 2015,20:10-16.
24. Liu Y, Zhang RY, Zhao J, Dong Z, Feng DY, Wu R, Shi M and Zhao G, Ginsenoside Rd Protects SH-SY5Y Cells against 1-Methyl-4-phenylpyridinium Induced Injury. *Int J Mol Sci*. 2015,16:14395-14408.
25. Bosoi CR, Tremblay M and Rose CF, Induction of systemic oxidative stress leads to brain oedema in portacaval shunted rats. *Liver Int*. 2014,34:1322-1329.
26. Jiang K, Wang W, Jin X, Wang Z, Ji Z and Meng G, Silibinin, a natural flavonoid, induces autophagy via ROS-dependent mitochondrial dysfunction and loss of ATP involving BNIP3 in human MCF7 breast cancer cells. *Oncol Rep*. 2015,33:2711-2718.
27. Perfeito R, Cunha-Oliveira T and Rego AC, Revisiting oxidative stress and mitochondrial dysfunction in the pathogenesis of Parkinson disease—resemblance to the effect of amphetamine drugs of abuse. *Free Radical Biology and Medicine*. 2012,53:1791-1806.
28. Ma Q, Role of nrf2 in oxidative stress and toxicity. *Annual review of pharmacology and toxicology*. 2013,53:401-426.
29. Kaspar JW, Niture SK and Jaiswal AK, Nrf2: INrf2 (Keap1) signaling in oxidative stress. *Free Radical Biology and Medicine*. 2009,47:1304-1309.